A Sparseness-Promoting Total-Variation Approach for the Design of Linear Clustered Phased Arrays

N. Anselmi, G. Gottardi, G. Oliveri, and A. Massa

Abstract

This work deals with the design of contiguously clustered linear phased arrays matching user-defined requirements in terms of far-field radiated pattern. Towards this aim, a novel total-variation compressive sensing (*TV-CS*) methodology has been developed and customized to the problem at hand such that the sparsity of the gradient of the array excitations is maximized. Thanks to such an approach, it is possible to obtain highly-performing designs with a reduced number of sub-arrays. Some numerical results are shown to assess the proposed *TV-CS* method when dealing with the clustering of linear arrays radiating Taylor patterns with different requirements on the side-lobe level (*SLL*).

Contents

1 Numerical Assessment

1.1 Taylor - $SLL = -40dB$ - $N = 100$

Array Geometry:

- Linear Array
- Number of Elements: $N = 100$
- Element Spacing: $\Delta L_{REF} = \lambda/2$
- Aperture Length: $L = 49.5\lambda$

Reference Pattern:

- Pencil Beam, Taylor
- Number of elements: $N = 100$
- Transition Index: $\overline{n} = 6$
- Sidelobe Ratio: $SLL = -40dB$

Pareto Parameters:

- Pattern Samples: $K \in \{4, 6, 8..., 20, 25, ..., 50, 60, 70, ..., 100, 300, 400, 500, 1000\}$
- Primary penalty parameter: $\mu \in \left\{2 \times 10^{-2}, 2 \times 10^{-1}, ..., 2 \times 10^{13}\right\}$
- Secondary penalty parameter: $\beta \in \left\{2 \times 10^{-2}, 2 \times 10^{-1}, ..., 2 \times 10^{13}\right\}$
- $m_t \in \left\{1 \times 10^{1}, 2 \times 10^{1}, 5 \times 10^{1}, 1 \times 10^{2}, 5 \times 10^{2}, 1 \times 10^{3}\right\}$
- $m_o \in \left\{5 \times 10^{0}, 5 \times 10^{1}, 1 \times 10^{2}, 5 \times 10^{2}, 1 \times 10^{3}\right\}$
- De-noising Tolerance: $\tau_c = 1 \times 10^{-2}$

TV-CS Parameters:

- Starting primary penalty parameter: $\mu_0 = \mu$ (default)
- Starting secondary penalty parameter: $\beta_0 = \beta$ (default)
- Outer stopping tolerance: $t_o = 1 \times 10^{-3}$ (default)
- Inner stopping tolerance: $t_i = 1 \times 10^{-3}$ (default)
- Isotropic/anisotropic TV flag: $\mathcal{F}_{TV} = 1$
- Negative/Positive signal: $\mathcal{F}_N = [false]$ (default)

- TV/L2 flag:$\mathcal{F}_{T2} = [false]$ (default)
- Real/Imaginary signal flag: $\mathcal{F}_R = [false]$ (default)
- Scaling Matrix A flag: $\mathcal{F}_A = [true]$ (default)
- Scaling Vector B flag: $\mathcal{F}_B = [true]$ (default)
- Guess Solution: $\mathcal{F}_G = 0$ (all zeroes)

RESULTS

Pareto Front:

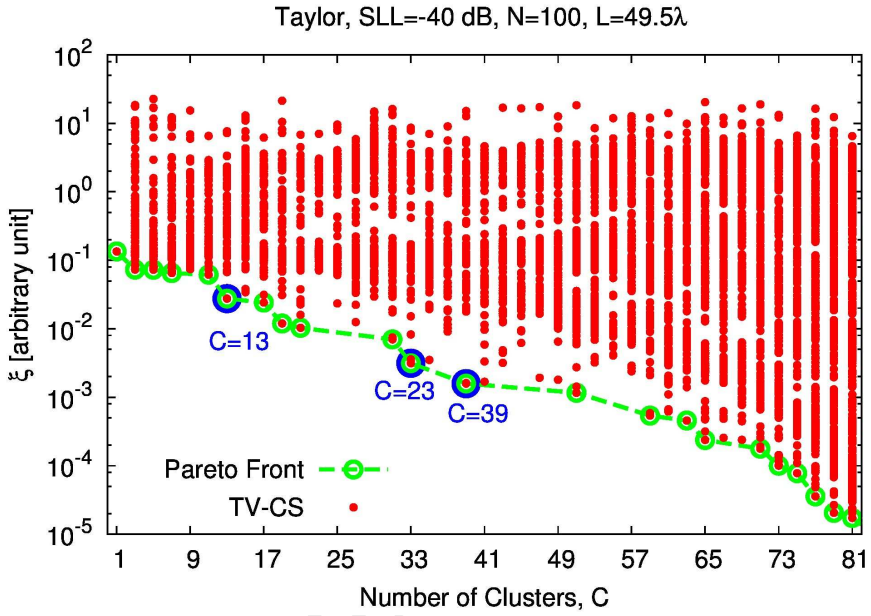

Figure 1: *Performance Assessment* (*Taylor Pattern*, $N = 100$, $SLL = -40$ dB, $d = 0.5\lambda$, $L = 49.5\lambda$)−Pareto front.

C	ξ	μ	β	K	m_t	m_o
13	2.76×10^{-2}	2×10^{-2}	2×10^{1}	200	5×10^{2}	1×10^{2}
33	3.14×10^{-3}	2×10^{-2}	2×10^{0}	100	1×10^{3}	5×10^{2}
39	1.59×10^{-3}	2×10^{-2}	2×10^{0}	1000	1×10^{3}	1×10^{2}

Table I: *Performance Assessment* (*Taylor Pattern*, $N = 100$, $SLL = -40$ dB, $d = 0.5\lambda$, $L = 49.5\lambda$)−Selected solutions.

Number of Clusters: $C = 13$

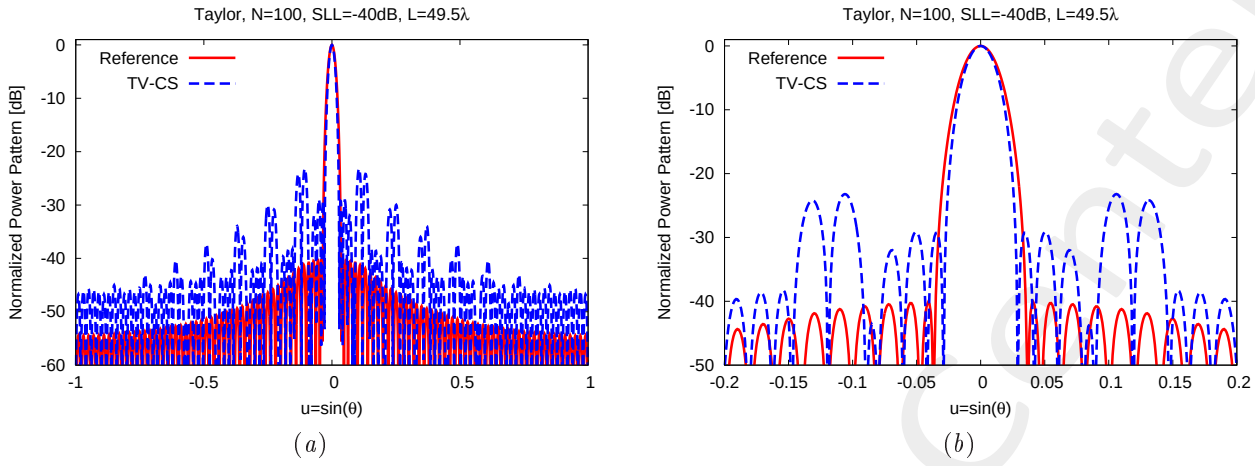

Figure 2: *Performance Assessment* (*Taylor Pattern*, $N = 100$, $SLL = -40$ dB, $d = 0.5\lambda$, $L = 49.5\lambda$, $C = 13$)-−Power pattern over the whole visible $u-$range (a) and a detail of the main lobe (b).

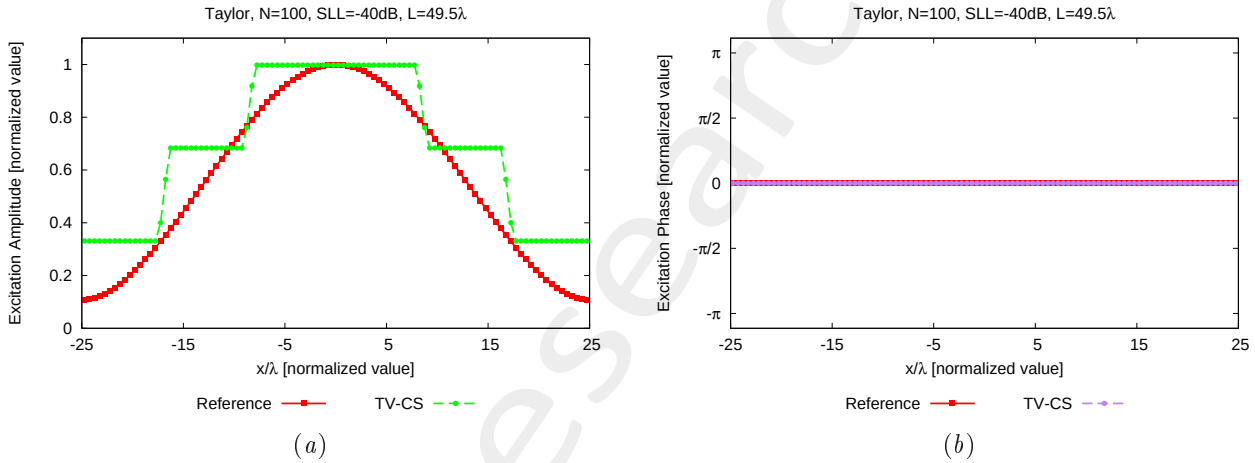

Figure 3: *Performance Assessment* (*Taylor Pattern*, $N = 100$, $SLL = -40$ dB, $d = 0.5\lambda$, $L = 49.5\lambda$, $C = 13$)-−Excitations amplitude (a) and phase (b).

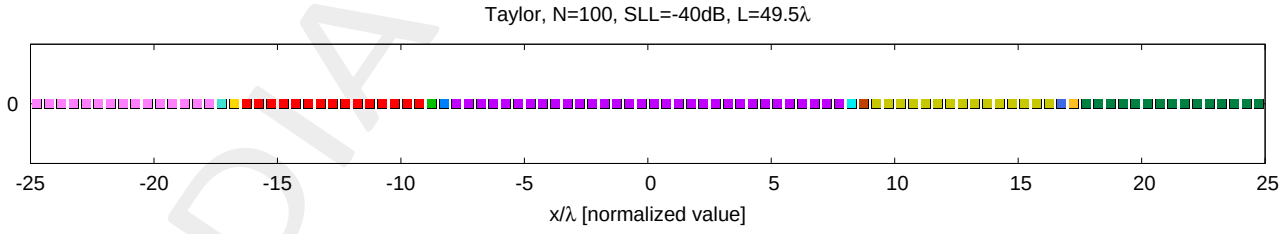

Figure 4: *Performance Assessment* (*Taylor Pattern*, $N = 100$, $SLL = -40$ dB, $d = 0.5\lambda$, $L = 49.5\lambda$, $C = 13$)-−Array elements clustering configuration.

	C	SLL [dB]	BW [deg]	$D_{\max}$ [dB]	DRR_{max}[dB]	$\xi \left[\times 10^{-2}\right]$
$Reference$	–	−40.00	1.4265	18.85	9.68	–
$TV-CS$	13	−23.20	1.2561	19.37	4.79	2.76

Table II: *Performance Assessment* (*Taylor Pattern*, $N = 100$, $SLL = -40$ dB, $d = 0.5\lambda$, $L = 49.5\lambda$, $C = 13$)-−Array Performance Indexes.

Number of Clusters: $C = 33$

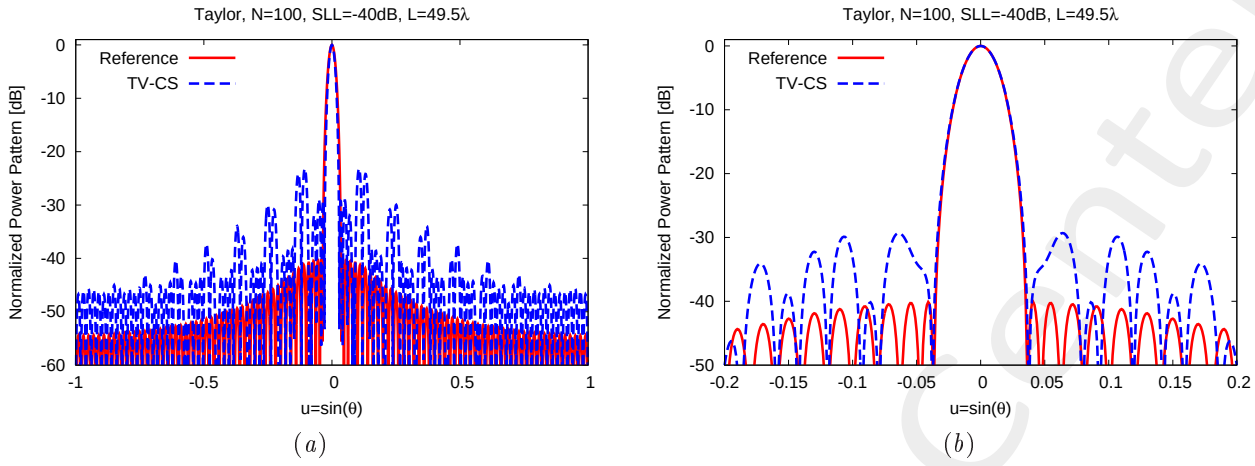

Figure 5: *Performance Assessment* (*Taylor Pattern*, $N = 100$, $SLL = -40$ dB, $d = 0.5\lambda$, $L = 49.5\lambda$, $C = 33$)-−Power pattern over the whole visible $u-$range (a) and a detail of the main lobe (b).

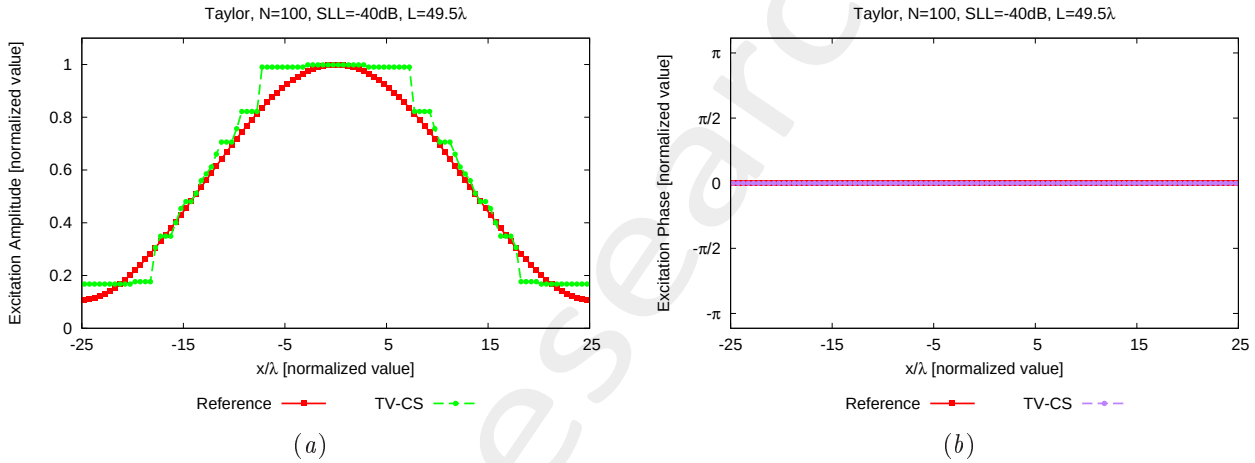

Figure 6: *Performance Assessment* (*Taylor Pattern*, $N = 100$, $SLL = -40$ dB, $d = 0.5\lambda$, $L = 49.5\lambda$, $C = 33$)-−Excitations amplitude (a) and phase (b).

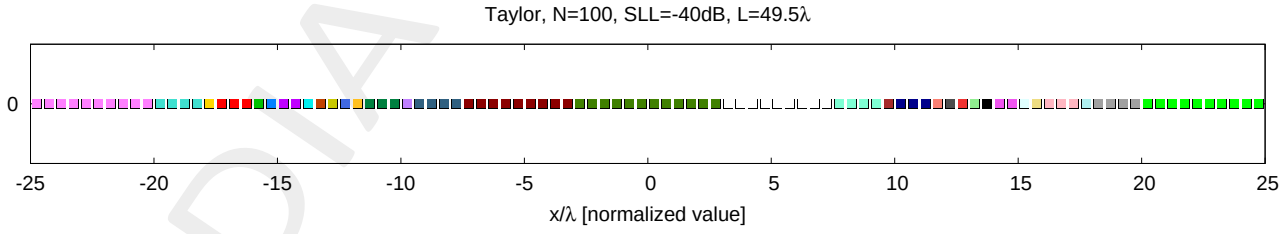

Figure 7: *Performance Assessment* (*Taylor Pattern*, $N = 100$, $SLL = -40$ dB, $d = 0.5\lambda$, $L = 49.5\lambda$, $C = 33$)-−Array elements clustering configuration.

	C	SLL [dB]	BW [deg]	$D_{\max}$ [dB]	DRR_{max}[dB]	ξ $[\times 10^{-3}]$
$Reference$	–	−40.00	1.4265	18.85	9.68	–
$TV-CS$	33	−29.30	1.4321	18.80	7.75	3.14

Table III: *Performance Assessment* (*Taylor Pattern*, $N = 100$, $SLL = -40$ dB, $d = 0.5\lambda$, $L = 49.5\lambda$, $C = 33$)-−Array Performance Indexes.

Number of Clusters: $C = 39$

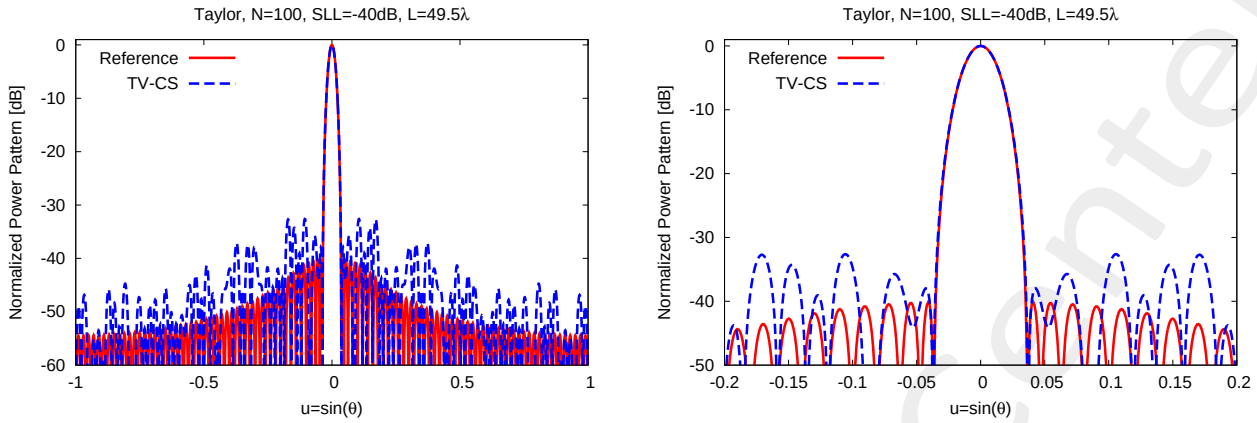

Figure 8: *Performance Assessment* (*Taylor Pattern*, $N = 100$, $SLL = -40$ dB, $d = 0.5\lambda$, $L = 49.5\lambda$, $C = 39$)-−Power pattern over the whole visible $u-$range (a) and a detail of the main lobe (b).

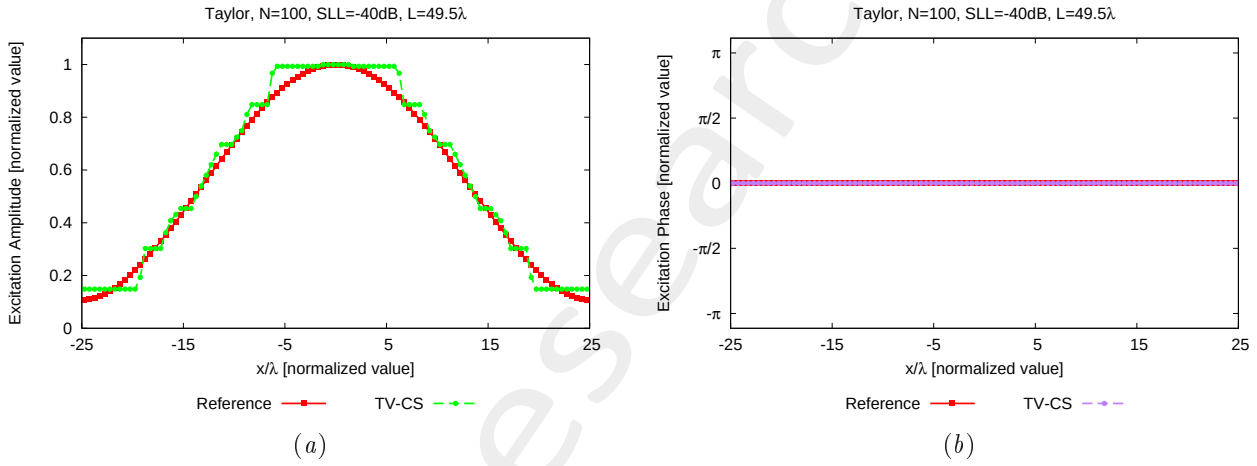

Figure 9: *Performance Assessment* (*Taylor Pattern*, $N = 100$, $SLL = -40$ dB, $d = 0.5\lambda$, $L = 49.5\lambda$, $C = 39$)-−Excitations amplitude (a) and phase (b).

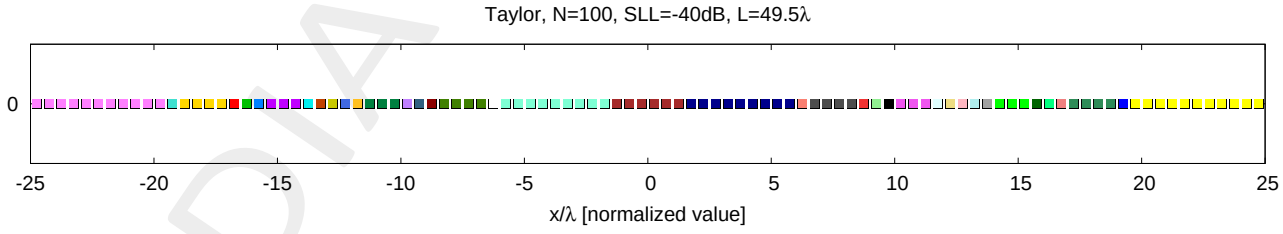

Figure 10: *Performance Assessment* (*Taylor Pattern*, $N = 100$, $SLL = -40$ dB, $d = 0.5\lambda$, $L = 49.5\lambda$, $C = 39$)-−Array elements clustering configuration.

	C	SLL [dB]	BW [deg]	$D_{\max}$ [dB]	DRR_{max}[dB]	$\xi \left[\times 10^{-3}\right]$
$Reference$	–	−40.00	1.4265	18.85	9.68	–
$TV-CS$	39	−32.62	1.4316	18.82	8.28	1.59

Table IV: *Performance Assessment* (*Taylor Pattern*, $N = 100$, $SLL = -40$ dB, $d = 0.5\lambda$, $L = 49.5\lambda$, $C = 39$)-−Array Performance Indexes.

1.2 Taylor - $SLL = -50dB$ - $N = 100$

Array Geometry:

- Linear Array
- Number of Elements: $N = 100$
- Element Spacing: $\Delta L_{REF} = \lambda/2$
- Aperture Length: $L = 49.5\lambda$

Reference Pattern:

- Pencil Beam, Taylor
- Number of elements: $N = 100$
- Transition Index: $\overline{n} = 6$
- Sidelobe Ratio: $SLL = -50dB$

Pareto Parameters:

- Pattern Samples: $K \in \{4, 6, 8..., 20, 25, ..., 50, 60, 70, ..., 100, 300, 400, 500, 1000\}$
- Primary penalty parameter: $\mu \in \left\{2 \times 10^{-2}, 2 \times 10^{-1}, ..., 2 \times 10^{13}\right\}$
- Secondary penalty parameter: $\beta \in \left\{2 \times 10^{-2}, 2 \times 10^{-1}, ..., 2 \times 10^{13}\right\}$
- $m_t \in \left\{1 \times 10^{1}, 2 \times 10^{1}, 5 \times 10^{1}, 1 \times 10^{2}, 5 \times 10^{2}, 1 \times 10^{3}\right\}$
- $m_o \in \left\{5 \times 10^{0}, 5 \times 10^{1}, 1 \times 10^{2}, 5 \times 10^{2}, 1 \times 10^{3}\right\}$
- De-noising Tolerance: $\tau_c = 1 \times 10^{-2}$

TV-CS Parameters:

- Starting primary penalty parameter: $\mu_0 = \mu$ (default)
- Starting secondary penalty parameter: $\beta_0 = \beta$ (default)
- Outer stopping tolerance: $t_o = 1 \times 10^{-3}$ (default)
- Inner stopping tolerance: $t_i = 1 \times 10^{-3}$ (default)
- Isotropic/anisotropic TV flag: $\mathcal{F}_{TV} = 1$
- Negative/Positive signal: $\mathcal{F}_N = [false]$ (default)
- TV/L2 flag:$\mathcal{F}_{T2} = [false]$ (default)

- Real/Imaginary signal flag: $\mathcal{F}_R = [false]$ (default)
- Scaling Matrix A flag: $\mathcal{F}_A = [true]$ (default)
- Scaling Vector B flag: $\mathcal{F}_B = [true]$ (default)
- Guess Solution: $\mathcal{F}_G = 0$ (all zeroes)

RESULTS

Pareto Front:

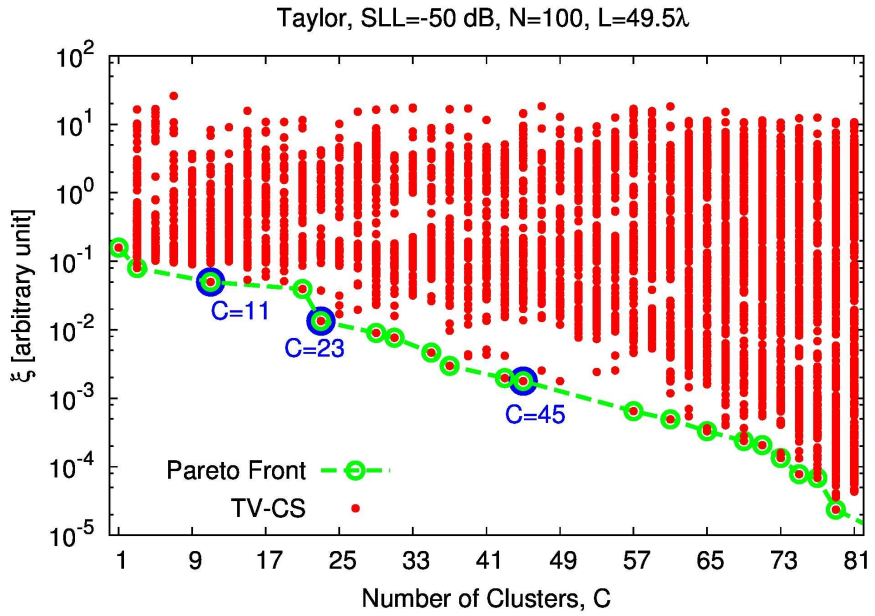

Figure 11: *Performance Assessment* (*Taylor Pattern*, $N = 100$, $SLL = -50$ dB, $d = 0.5\lambda$, $L = 49.5\lambda$)−Pareto front.

C	ξ	μ	β	K	m_t	m_o
11	5.00×10^{-2}	2×10^{-2}	2×10^{1}	200	5×10^{2}	5×10^{1}
23	1.34×10^{-2}	2×10^{-1}	2×10^{1}	80	5×10^{2}	5×10^{1}
45	1.78×10^{-3}	2×10^{-2}	2×10^{0}	200	1×10^{3}	5×10^{2}

Table V: *Performance Assessment* (*Taylor Pattern*, $N = 100$, $SLL = -50$ dB, $d = 0.5\lambda$, $L = 49.5\lambda$)−Selected solutions.

Number of Clusters: $C = 11$

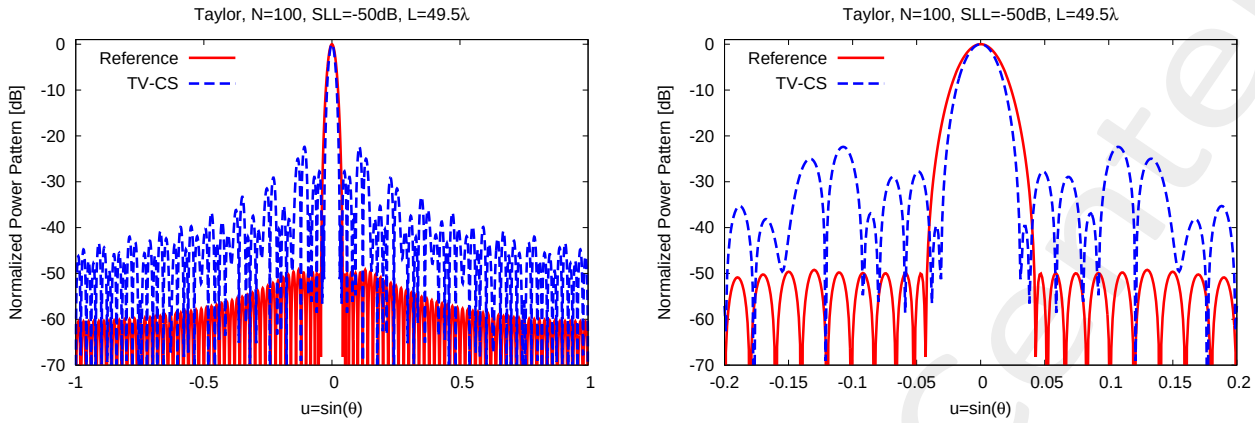

Figure 12: *Performance Assessment* (*Taylor Pattern*, $N = 100$, $SLL = -50$ dB, $d = 0.5\lambda$, $L = 49.5\lambda$, $C = 11$)-−Power pattern over the whole visible $u-$range (a) and a detail of the main lobe (b).

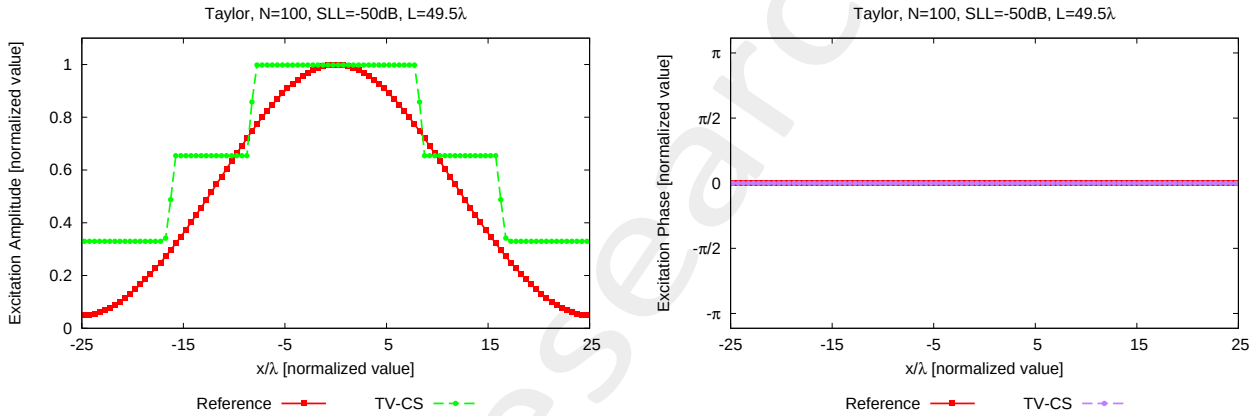

Figure 13: *Performance Assessment* (*Taylor Pattern*, $N = 100$, $SLL = -50$ dB, $d = 0.5\lambda$, $L = 49.5\lambda$, $C = 11$)-−Excitations amplitude (a) and phase (b).

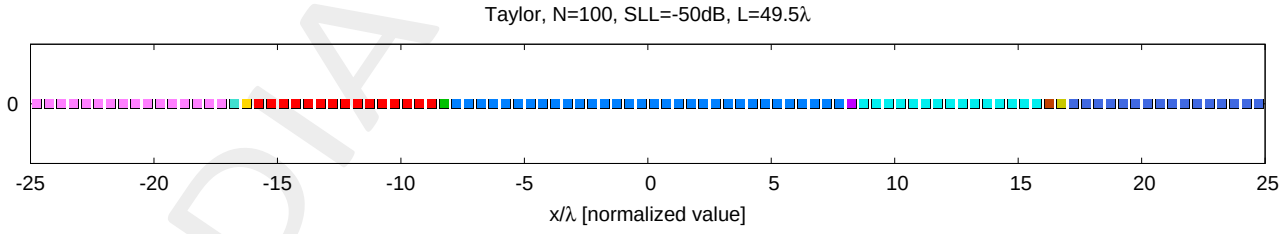

Figure 14: *Performance Assessment* (*Taylor Pattern*, $N = 100$, $SLL = -50$ dB, $d = 0.5\lambda$, $L = 49.5\lambda$, $C = 11$)-−Array elements clustering configuration.

	C	SLL [dB]	BW [deg]	$D_{\max}$ [dB]	DRR_{max}[dB]	$\xi \left[\times 10^{-2}\right]$
$Reference$	–	−50.00	1.5513	18.47	13.08	–
$TV-CS$	11	−22.39	1.2681	19.30	4.81	5.00

Table VI: *Performance Assessment* (*Taylor Pattern*, $N = 100$, $SLL = -50$ dB, $d = 0.5\lambda$, $L = 49.5\lambda$, $C = 11$)-−Array Performance Indexes.

Number of Clusters: $C = 23$

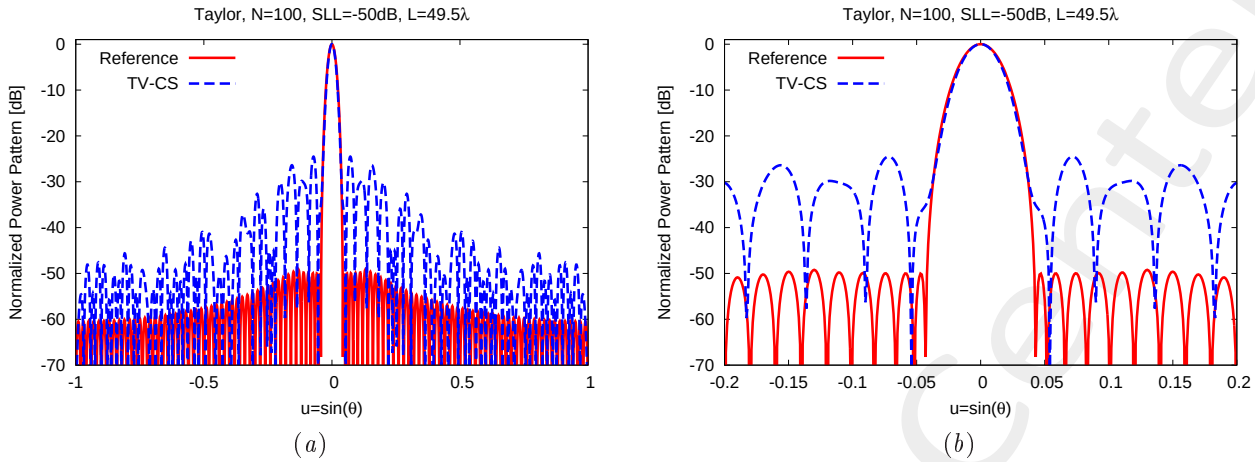

Figure 15: *Performance Assessment* (*Taylor Pattern*, $N = 100$, $SLL = -50$ dB, $d = 0.5\lambda$, $L = 49.5\lambda$, $C = 23$)-−Power pattern over the whole visible $u-$range (a) and a detail of the main lobe (b).

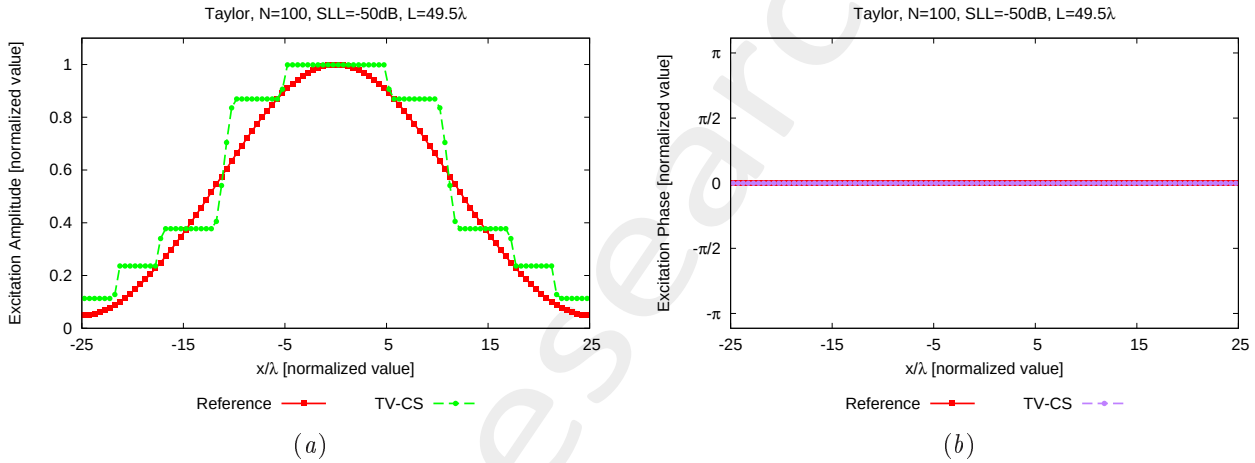

Figure 16: *Performance Assessment* (*Taylor Pattern*, $N = 100$, $SLL = -50$ dB, $d = 0.5\lambda$, $L = 49.5\lambda$, $C = 23$)-−Excitations amplitude (a) and phase (b).

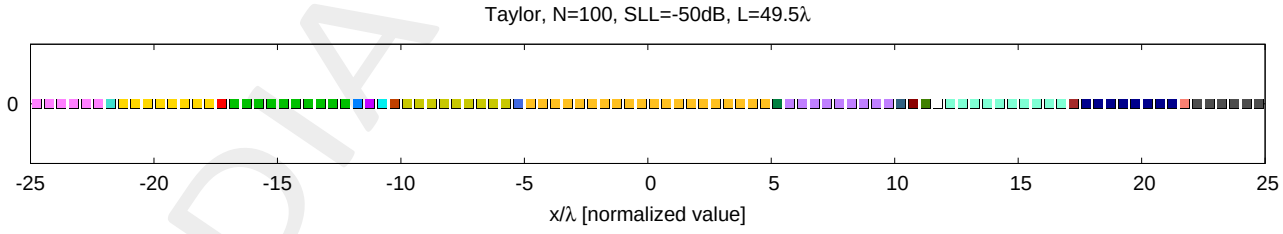

Figure 17: *Performance Assessment* (*Taylor Pattern*, $N = 100$, $SLL = -50$ dB, $d = 0.5\lambda$, $L = 49.5\lambda$, $C = 23$)-−Array elements clustering configuration.

	C	SLL [dB]	BW [deg]	$D_{\max}$ [dB]	DRR_{max}[dB]	$\xi \left[\times 10^{-2}\right]$
$Reference$	–	−50.00	1.5513	18.47	13.08	–
$TV-CS$	23	−24.52	1.4593	18.67	9.46	1.34

Table VII: *Performance Assessment* (*Taylor Pattern*, $N = 100$, $SLL = -50$ dB, $d = 0.5\lambda$, $L = 49.5\lambda$, $C = 23$)-−Array Performance Indexes.

Number of Clusters: $C = 45$

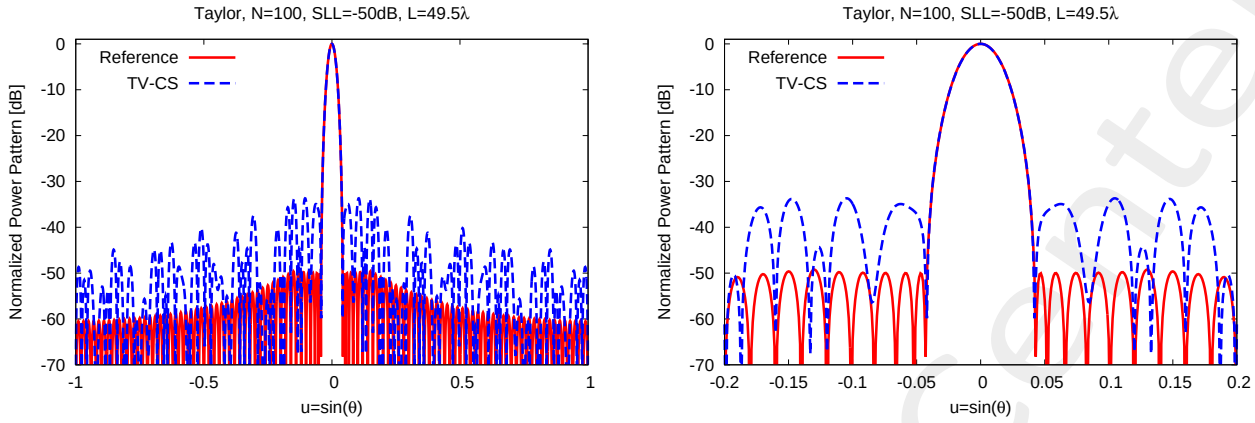

Figure 18: *Performance Assessment* (*Taylor Pattern*, $N = 100$, $SLL = -50$ dB, $d = 0.5\lambda$, $L = 49.5\lambda$, $C = 45$)-−Power pattern over the whole visible $u-$range (a) and a detail of the main lobe (b).

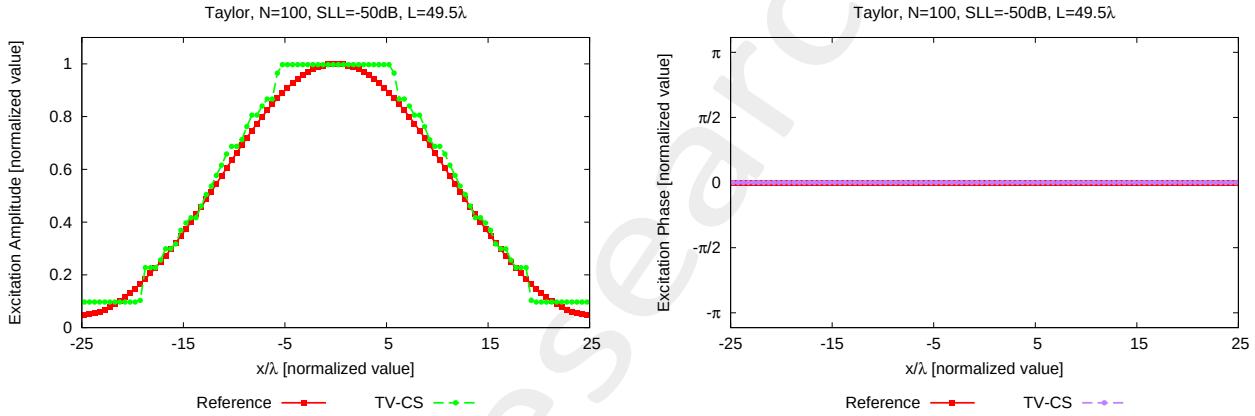

Figure 19: *Performance Assessment* (*Taylor Pattern*, $N = 100$, $SLL = -50$ dB, $d = 0.5\lambda$, $L = 49.5\lambda$, $C = 45$)-−Excitations amplitude (a) and phase (b).

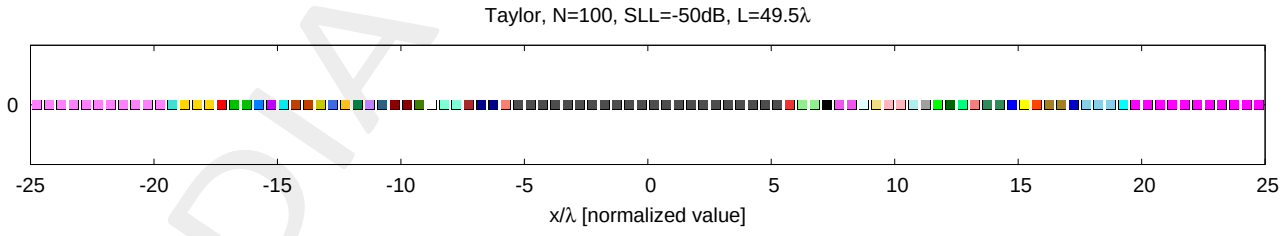

Figure 20: *Performance Assessment* (*Taylor Pattern*, $N = 100$, $SLL = -50$ dB, $d = 0.5\lambda$, $L = 49.5\lambda$, $C = 45$)-−Array elements clustering configuration.

	C	SLL [dB]	BW [deg]	$D_{\max}$ [dB]	DRR_{max}[dB]	$\xi\ [\times 10^{-3}]$
$Reference$	–	−50.00	1.5513	18.47	13.08	–
$TV-CS$	45	−33.68	1.5393	18.49	10.11	1.78

Table VIII: *Performance Assessment* (*Taylor Pattern*, $N = 100$, $SLL = -50$ dB, $d = 0.5\lambda$, $L = 49.5\lambda$, $C = 45$)−Array Performance Indexes.

References

[1] P. Rocca, G. Oliveri, R. J. Mailloux, and A. Massa, "Unconventional phased array architectures and design methodologies - A Review," *Proc. IEEE*, vol. 104, no. 3, pp. 544-560, Mar. 2016.

[2] G. Oliveri, G. Gottardi, F. Robol, A. Polo, L. Poli, M. Salucci, M. Chuan, C. Massagrande, P. Vinetti, M. Mattivi, R. Lombardi, and A. Massa, "Co-design of unconventional array architectures and antenna elements for *5G* base stations," *IEEE Trans. Antennas Propag.*, vol. 65, no. 12, pp. 6752-6767, Dec. 2017.

[3] N. Anselmi, P. Rocca, M. Salucci, and A. Massa, "Irregular phased array tiling by means of analytic schemata-driven optimization," *IEEE Trans. Antennas Propag.*, vol. 65, no. 9, pp. 4495-4510, Sep. 2017.

[4] G. Oliveri, "Multi-beam antenna arrays with common sub-array layouts," *IEEE Antennas Wireless Propag. Lett.*, vol. 9, pp. 1190-1193, 2010.

[5] P. Rocca, R. Haupt, and A. Massa, "Sidelobe reduction through element phase control in sub-arrayed array antennas," *IEEE Antennas Wireless Propag. Lett.*, vol. 8, pp. 437-440, 2009.

[6] P. Rocca, L. Manica, R. Azaro, and A. Massa, "A hybrid approach for the synthesis of sub-arrayed monopulse linear arrays," *IEEE Trans. Antennas Propag.*, vol. 57, no. 1, pp. 280-283, Jan. 2009.

[7] G. Oliveri, P. Rocca, and A. Massa, "Reliable diagnosis of large linear arrays - a Bayesian compressive sensing approach," *IEEE Trans. Antennas Propag.*, vol. 60, no. 10, pp. 4627-4636, Oct. 2012.

[8] A. Massa, P. Rocca, and G. Oliveri, "Compressive sensing in electromagnetics - A review," *IEEE Antennas Propag. Mag.*, pp. 224-238, vol. 57, no. 1, Feb. 2015.

[9] G. Oliveri, M. Salucci, N. Anselmi, and A. Massa, "Compressive sensing as applied to inverse problems for imaging: theory, applications, current trends, and open challenges," *IEEE Antennas Propag. Mag.,* vol. 59, no. 5, pp. 34-46, Oct. 2017.

[10] P. Rocca, M. A. Hannan, M. Salucci, and A. Massa, "Single-snapshot DoA estimation in array antennas with mutual coupling through a multi-scaling Bayesian compressive sensing strategy," *IEEE Trans. Antennas Propag.*, vol. 65, no. 6, pp. 3203-3213, Jun. 2017.

[11] L. Poli, G. Oliveri, P. Rocca, M. Salucci, and A. Massa, "Long-distance WPT unconventional arrays synthesis," *J. Electromagn. Waves Appl.*, vol. 31, no. 14, pp. 1399-1420, Jul. 2017.

[12] G. Oliveri, M. Salucci, and A. Massa, "Synthesis of modular contiguously clustered linear arrays through a sparseness-regularized solver," *IEEE Trans. Antennas Propag.*, vol. 64, no. 10, pp. 4277-4287, Oct. 2016.

[13] F. Viani, G. Oliveri, and A. Massa, "Compressive sensing pattern matching techniques for synthesizing planar sparse arrays," *IEEE Trans. Antennas Propag.*, vol. 61, no. 9, pp. 4577-4587, Sept. 2013.

[14] G. Oliveri and A. Massa, "Bayesian compressive sampling for pattern synthesis with maximally sparse non-uniform linear arrays," *IEEE Trans. Antennas Propag.*, vol. 59, no. 2, pp. 467-481, Feb. 2011.

[15] N. Anselmi, G. Oliveri, M. A. Hannan, M. Salucci, and A. Massa, "Color compressive sensing imaging of arbitrary-shaped scatterers," *IEEE Trans. Microw. Theory Techn.*, vol. 65, no. 6, pp. 1986-1999, Jun. 2017.

[16] N. Anselmi, G. Oliveri, M. Salucci, and A. Massa, "Wavelet-based compressive imaging of sparse targets," *IEEE Trans. Antennas Propag.*, vol. 63, no. 11, pp. 4889-4900, Nov. 2015.

[17] G. Oliveri, N. Anselmi, and A. Massa, "Compressive sensing imaging of non-sparse 2D scatterers by a total-variation approach within the Born approximation," *IEEE Trans. Antennas Propag.*, vol. 62, no. 10, pp. 5157-5170, Oct. 2014.

[18] N. Anselmi, G. Gottardi, G. Oliveri, and A. Massa, "A total-variation sparseness-promoting method for the synthesis of contiguously clustered linear architectures" *IEEE Trans. Antennas Propag.*, vol. 67, no. 7, pp. 4589-4601, Jul. 2019.

[19] M. Salucci, A. Gelmini, G. Oliveri, and A. Massa, "Planar arrays diagnosis by means of an advanced Bayesian compressive processing," *IEEE Tran. Antennas Propag.*, vol. 66, no. 11, pp. 5892-5906, Nov. 2018.